Journal of Materiomics 11 (2025) 100935

Contents lists available at ScienceDirect

Journal of Materiomics

journal homepage: www.journals.elsevier.com/journal-of-materiomics/

Research paper

Air-stable silicon hybrid solar cells constructed *via* hydrophobic polymer film

Qi Geng [a, 1], Zhen Liu [a, 1], Yuzhou Liu [a], Zhe Wang [a], Zhongliang Gao [c], Xin Sun [a], Yingfeng Li [a], Lei Chen [b], Xiaojun Lv [a], Meicheng Li [a, *]

[a] State Key Laboratory of Alternate Electrical Power System with Renewable Energy Sources, School of New Energy, North China Electric Power University, Beijing, 102206, China
[b] School of Mathematics and Physics, North China Electric Power University, Beijing, 102206, China
[c] School of Electrical and Electronic Engineering, Shandong University of Technology, Zibo, 255000, Shandong, China

ARTICLE INFO

Article history:
Received 12 June 2024
Received in revised form
27 July 2024
Accepted 1 August 2024
Available online 31 August 2024

Keywords:
Hydrophobic
PEDOT
Si
Hybrid
Solar cells

ABSTRACT

Silicon (Si) hybrid solar cells have advantages of solution manufacturing process and the potential for achieving low-cost fabrication compared to crystalline Si solar cells. However, the functional layer prepared by solution method usually absorbs water molecules from the air, posing a challenge to the stability of the device. Here, a PEDOT derivative, PEDOT:A, was *in situ* prepared through the introduction of a fluoropolymer, yielding a strongly hydrophobic film that was assembled into a PEDOT:A/Si hybrid solar cell. The PEDOT:A/Si hybrid solar cells retained 90% of its initial performance after storage in the air for 300 h, while PEDOT:PSS only retained 60% with identical device structure. Meanwhile, first principles calculations indicate that the binding energy between fluoropolymer and water molecule was 3.48 kJ/mol, whereas the binding energy between PSS and water molecule was −5.76 kJ/mol. Benefiting from the weak interaction between fluoropolymer and water molecule, the contact angle of water on PEDOT:A film was 100.84°. After optimization, PEDOT:A/Si hybrid solar cells with ITO achieved a power conversion efficiency of 6.43%, retained 97% of its initial efficiency after testing under same conditions. The development of air-stable hybrid device technology is promising in opening up practical applications of low-cost Si based solar cells.

1. Introduction

Silicon (Si) hybrid solar cells are typically fabricated by spin-coating functional materials on the Si surface [1–3]. The fabrication process of crystalline silicon (Si) solar cells usually requires the support of capital-intensive equipment and involves high temperature and complex depositing processes. Therefore, it has the merits of solution manufacturing process and the potential for achieving low-cost fabrication [4–8] compared to crystalline Si solar cells. Furthermore, through the optimization of functional layers, the efficiency of Si hybrid solar cells [9–15] has gradually approached the levels of crystalline Si solar cells. Among a wide range of functional materials, PEDOT has become a desirable candidate for achieving various functions in the fields of photovoltaics [16–19], quantum dot light emitting diodes (QLEDs) [20,21], and energy storage [22,23] due to its good electric conductivity, thermal stability, and high transmittance. However, electrochemical polymerization makes it challenging for PEDOT to form film on non-conductive substrates. Due to solubility limitations [24,25], adopting chemical oxidative polymerization is also arduous for forming PEDOT films on diverse substrates, which further restricts its widespread application. Fortunately, a uniformly dispersed aqueous solution of PEDOT can be prepared with the use of water-soluble polystyrene sulfonic acid (PSS) as a template [26]. This enables PEDOT to achieve film formation on different substrates through spin-coating or other methods, so that it can better meet the requirements of solution process.

Despite a uniformly dispersed PEDOT solution was achieved by using PSS as a template, after film formation, the hygroscopic nature of PSS components still impairs the stability of Si hybrid solar cells in the air. By spin-coating PEDOT:PSS solution on the Si surface

* Corresponding author.
E-mail address: mcli@ncepu.edu.cn (M. Li).
Peer review under responsibility of The Chinese Ceramic Society.
[1] Qi Geng and Zhen Liu contributed equally.

https://doi.org/10.1016/j.jmat.2024.100935

to construct hybrid solar cells and monitoring the changes in device performance under different humidity environments. It was found that the continuous degradation of device performance was mainly caused by water molecules in the air [27]. Using 2,2′,7,7′-tetrakis (N,N-di-4-methoxyphenylamino) 9,9′-spirobifluorene (Spiro-OMeTAD) can also construct Si hybrid solar cells, but, in order to improve the efficiency of devices, PEDOT:PSS film was spin-coated on Spiro-OMeTAD layer [28]. Meanwhile, it was also discovered that the performance of the device in the air decays more severely compared to a dry atmosphere. Therefore, to mitigate the damage to the stability of Si hybrid solar cells caused by the hygroscopic nature of PSS components in PEDOT:PSS film, a lot of research has been carried out. After spin-coating a water-insoluble diethyl phthalate (DEP) on PEDOT:PSS film, the PCE of the device retains 90% of its initial efficiency after storage in the air for 300 h [9]. Thermal evaporation of copper iodide (CuI) on PEDOT:PSS film can also retain 65% of the initial efficiency of the device after storage for 300 h in the air [29]. The stability of Si hybrid solar cells can also be enhanced by improving the hydrophobicity of PEDOT:PSS film *via* rational doping of PEDOT:PSS solution. Isobutyltriethoxysilane (IBTEO) was selected as an additive to be added in PEDOT:PSS solution for constructing Si hybrid heterojunction solar cells. It was detected that after storage in the air for 300 h, the PCE of the device retained 78% of its initial efficiency [14]. By doping waterborne acrylic resin (WA) in PEDOT:PSS solution, the device retained more than 80% of its initial efficiency after storage for 200 h in the air [30]. In addition, developing other functional materials to replace PEDOT:PSS film is also a method for constructing stable Si hybrid solar cells. TED-Li was investigated by drop-coated it on Si-nanotips to construct nanostructure Si hybrid solar cells, which retained 90% of its initial efficiency for nearly a month of air stability monitoring [31]. The aforementioned studies indicate that appropriate surface treatments and the utilization of additives can attenuate the effect of water molecules in the air on PEDOT:PSS film, thus improving the stability of the device. On the other hand, designing new material to substitute for PEDOT:PSS film also represents a valid way for constructing stable Si hybrid solar cells. Although PSS can be used to disperse PEDOT, the resulting films are not hydrophobic. Despite this, research on dispersing PEDOT without the use of PSS and preparing hydrophobic films to construct stable Si hybrid solar cells remains neglected.

In this work, a PEDOT derivative, PEDOT:A, was prepared through the introduction of a fluoropolymer. The PEDOT:A film shows strongly hydrophobic and PEDOT:A/Si hybrid solar cells were constructed through PEDOT:A film. The PEDOT:A/Si hybrid solar cells retained 90% of its initial efficiency after storage in the air for 300 h compared to 60% of PEDOT:PSS, under identical conditions. Further, first principles calculations suggest that the weak interaction between fluoropolymer and water molecule results in the contact angle of water on PEDOT:A film exceeding 100°, making it more stable in water for a long time. Meanwhile, with the optimization of ITO, the PEDOT:A/Si hybrid solar cells achieved a power conversion efficiency (PCE) of 6.43%.

2. Experimental section

2.1. Materials

EDOT and $FeCl_3$ were purchased from Acros and aladdin. Aquivion D98 and Dialysis membranes (500 Da) were bought from Beijing Apsilon and Yobios. PEDOT:PSS solution is Clevios PH1000 of Heraeus. Triton® X-100 (TX-100) and Ethylene glycol, 99%, were purchased from Alfa and Innochem. Radial (100) polished single-side n-Si wafer was purchased from Tianjin Upward Technology Development Co., Ltd with a resistivity of 2–4 Ω·cm and a thickness of 500 μm.

2.2. PEDOT:A solution synthesis process

Firstly, 0.38 mmol EDOT and 0.21 mmol Aquivion, and 15 mL water were mixed and stirred for 2 h. Next, 0.75 mmol $FeCl_3$ was added to the above solution and stirred for 24 h to oxidize EDOT to PEDOT. Thirdly, the dark blue solution was transferred to the dialysis membrane for purification. Then, the dark blue solution was collected and centrifugation. Finally, the product was collected and mixed with ethanol by shear force and used ultrasonic cell crusher for 6 h.

2.3. PEDOT:A/Si hybrid solar cell fabrication

The Si wafer was cut into 1 cm × 1 cm by a laser dicing machine. And then the Si wafer was cleaned in acetone, ethanol and deionized (DI) water for 10 min each, and dry the Si wafer with nitrogen. After the cleaning process, the 5% hydrofluoric acid was used to remove the native oxide layer on the Si surface and then cleaned with DI water. Ethylene glycol (EG) was added into PEDOT:A solution and the ratio by volume of EG and PEDOT:A was 1:30 and stirred adequately. The PEDOT:A solution was spin-coated on Si wafer by 7000 r/min and annealed at 120 °C for 15 min, and ITO was sputtered on PEDOT:A film about 70 nm. The 0.25% (in mass) TX-100 was mixed with PEDOT:PSS solution, and stirred adequately. Ag electrode was deposited onto the PEDOT:PSS and PEDOT:A film through a shadow mask by magnetron sputtering with a thickness of 200 nm. An Ag film was prepared as rear electrode with a thickness of 100 nm. Finally, the cell was cut into 0.5 cm × 0.5 cm for testing.

2.4. Characterization

The solar simulator (Keithley 2400, AM 1.5G, 100 mW/cm^2) was used to test the current density and voltage (J–V) characteristics. The morphology of PEDOT:A film was characterized by Hitachi SU8100 cold field Scanning Electron Microscopy (SEM). Raman spectra of PEDOT:A film and PEDOT:PSS film was tested on Si substrate. X-ray Photoelectron Spectroscopy (XPS) and Ultraviolet Photoelectron Spectroscopy (UPS) were used to measure the optoelectronic information of PEDOT:A films. The optical properties of PEDOT:A film on ITO were obtained by UV2600i. Conductive AFM of PEDOT:A and PEDOT:PSS film was performed by atomic force microscopy (AFM). The reflectivity spectra were detected by Enli technology QE-R test system.

2.5. Calculate method

To assess the binding energies between Aquivion, PSS, Nafion, and water molecule, we streamline the interactions where a water molecule binds with Aquivion, PSS, and Nafion featuring a simplified short chain backbone ($m = 1$, $n = 1$). For Aquivion and Nafion, the water molecule was positioned adjacent to the C–F_2 backbond; for PSS, it was placed near the SO_3H^- fragment. All density functional theory (DFT) calculations are performed using Gaussian 16 suite of programs.

3. Results and discussion

3.1. Indication for the synthesis of PEDOT:A polymer

At the beginning, to verify the successful polymerization of PEDOT derivative, PEDOT:A, the Raman spectra of PEDOT:A and PEDOT:PSS film was presented in Fig. 1a. After comparing the

spectrum of PEDOT:A film with that of PEDOT:PSS film, it was found that they closely resemble each other, indicating that the two materials were nearly identical. The peaks at 438, 576 cm^{-1}, and 986 cm^{-1} are associated with the deformation of oxyethylene ring. The peaks at 696, 854 cm^{-1}, and 1101 cm^{-1} are in connection with symmetric C–S–C and C–O–C stretching [32]. The peaks at 1259, 1366 cm^{-1}, and 1433 cm^{-1} correspond to the C_α–C_α, C_β–C_β, and $C_\alpha = C_\beta$ stretching vibrations, respectively [33,34]. Meanwhile, surface chemical analysis of PEDOT:A film was performed by XPS. As shown in Fig. 1b, the spectra are dominated by the signals of sulfur, carbon, oxygen, and fluorine. The S 2p and F 1s core level spectra of PEDOT:A film was also shown in Fig. 1c and d. The binding energy of 168.8 eV can be ascribed to the sulfonate groups of fluoropolymer-Aquivion. The binding energy of 688.8 eV corresponds to fluorine, which also belongs to fluoropolymer-Aquivion. The sulfur atoms of the thiophene moiety in the PEDOT show double peaks at lower binding energies of 164 eV and 165.1 eV, respectively [35,36]. These characteristic response peaks indicate the successful polymerization of PEDOT:A.

3.2. Properties of PEDOT:A solution and film

When constructing Si hybrid devices directly through spin-coating or other solution methods, the selected functional materials should meet the following criteria. Firstly, they should be able to form film uniformly on the Si surface with good transmittance. Additionally, the band position needs to be compatible with Si to ensure the smooth transport of carriers. Thus, the contact angle of PEDOT:A solution and surface morphology images of PEDOT:A film on different substrates were shown in Fig. 2. Firstly, the contact angle of PEDOT:A solution and PEDOT:PSS solution on the Si surface was tested, as shown in Fig. 2a–2b. It can be observed that the contact angle of PEDOT:A without any surfactant added was 16.47°, which was lower than 76.4° of PEDOT:PSS. On the contrary, for PEDOT:PSS, in order to form film on the Si surface by spin-coating, surfactants are typically required. Therefore, the TX-100 was added to PEDOT:PSS solution to enhance its wettability on the Si surface. In Fig. S1a, the contact angle of PEDOT:PSS with TX-100 was 37.61°, which is still larger than PEDOT:A. The main reason for this difference is the PEDOT:A was dispersed in ethanol, but the PEDOT:PSS is a water-dispersed solution. To further demonstrate the good wettability and film formation properties of PEDOT:A solution, the contact angle and surface morphology images on transparent conductive substrates were also presented. In Fig. 2d and e, the contact angles of PEDOT:A solution on UV-treated and non-treated FTO substrates were 9.04° and 18.36°, respectively. The contact angles of PEDOT:A solution on UV-treated and non-treated ITO substrates also showed a similar trend, in Fig. 2g–2h, and the value of contact angle statistical chart was shown in Fig. 2j. The surface morphology images of PEDOT:A film on different substrates including Si, FTO, and ITO were also displayed in Fig. 2c, f, and Fig. 2i, exhibiting a uniform surface. In order to construct devices, EG was added to the PEDOT:A solution, and the contact angle on the Si surface was 13.46°, as shown in Fig. S1b, slightly lower than the intrinsic solution. The surface morphology image of PEDOT:A film was also shown in Fig. S2, and there was no obvious change in surface morphology after adding EG. Based on these requirements, the transmittance of PEDOT:A film was also shown in Fig. S3a. It can be seen that the PEDOT:A film maintains a transmittance of more than 80%.

3.3. Construction and performance of PEDOT:A/Si hybrid solar cells

In addition, the band position was further performed, after

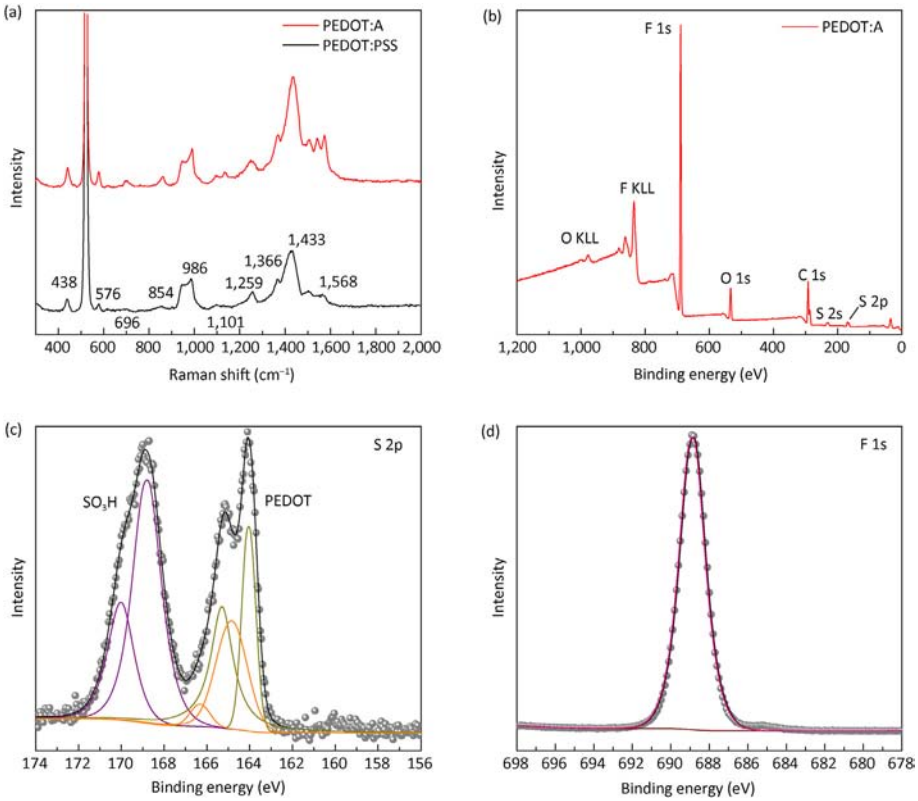

Fig. 1. Raman and XPS spectra of PEDOT:A film. (a) Raman spectra of PEDOT:A and PEDOT:PSS film. (b) Wide scan XPS analysis of PEDOT:A film. (c) S 2p and (d) F 1s core level spectra of PEDOT:A film.

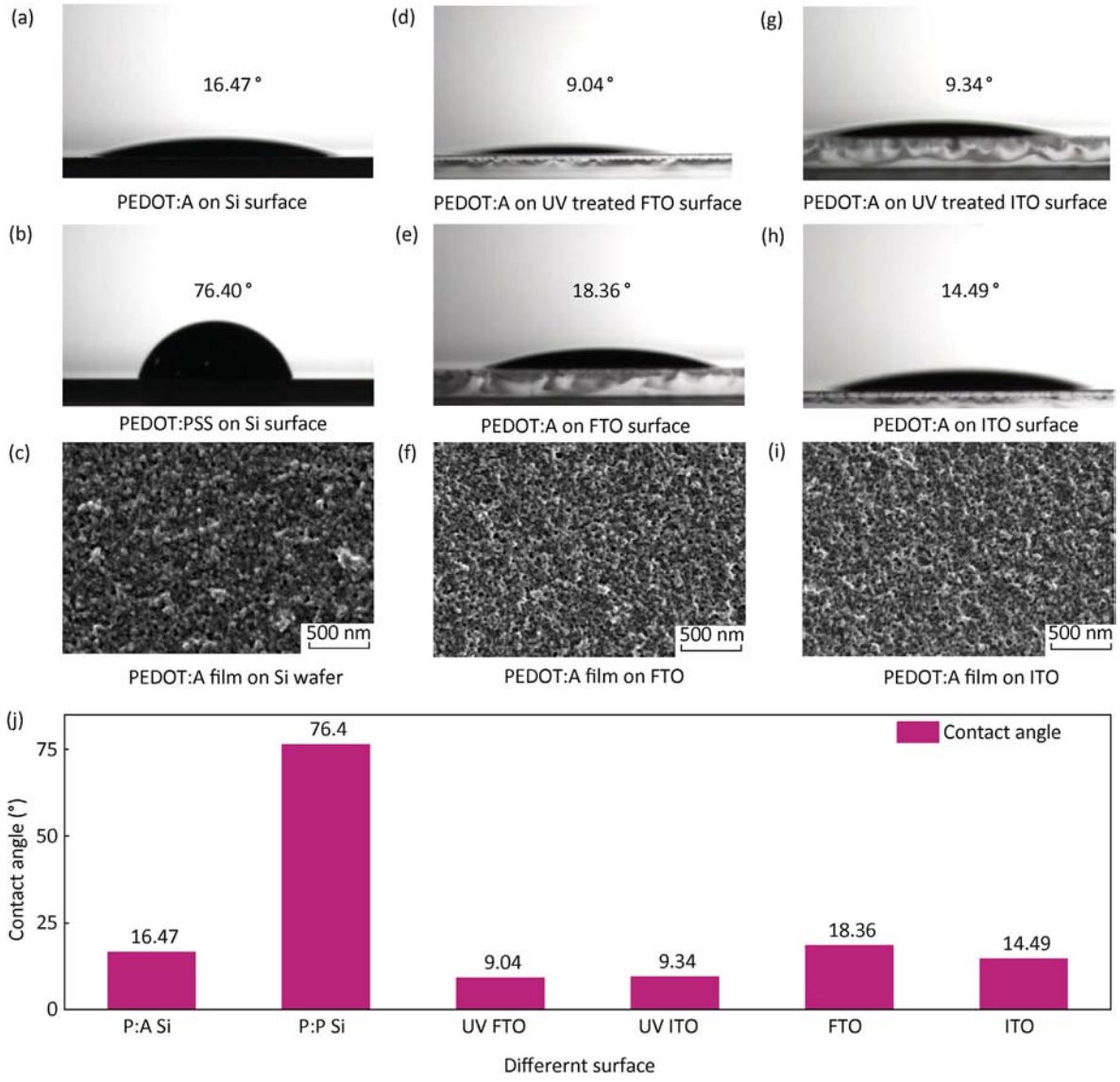

Fig. 2. Contact angle images and surface scanning electron microscope (SEM) images of different solution and PEDOT:A film on different substrates. (a) Contact angle image of PEDOT:A solution on the Si surface. (b) Contact angle image of PEDOT:PSS solution on the Si surface. (c) Surface scanning electron microscope (SEM) image of PEDOT:A film on the Si surface. (d) Contact angle image of PEDOT:A solution on UV-treated FTO surface and (e) not-treated FTO surface. (f) Surface scanning electron microscope (SEM) image of PEDOT:A film on FTO surface. (g) Contact angle image of PEDOT:A solution on UV-treated ITO surface and (h) not-treated ITO surface. (i) Surface scanning electron microscope (SEM) image of PEDOT:A film on ITO surface. (j) The value of contact angle statistical chart with different solution on different substrate surface.

obtaining the original data from UPS, calibrating, coordinating, transforming, and then calculating by formula (1),

$$\Phi = h\nu - \left(E_{\text{Cutoff}} - E_{\text{Fermi}}\right) \quad (1)$$

where Φ is work function, $h\nu$ is incident photon energy, here is 21.2 eV, E_{Cutoff} is the cut-off edge, and E_{Fermi} is the Fermi level after calibration. The values of VBM, W_F, and bandgap (E_g) of PEDOT:A film were 0.35, 4.8 eV, and 1.93 eV, respectively, and were obtained from Fig. 3a and Fig. S3b of the UPS and absorbance spectrum. It can also be calculated that the conduction band (E_C) of PEDOT:A film is 3.22 eV, which was obtained from the formula of $E_C{=}W_F$ (Φ) + VBM$-E_g$. Furthermore, the valence band (E_V) was also calculated as 5.15 eV according to the above results in Fig. 3b. It can be derived that, the band position of PEDOT:A film is compatible with Si, which can facilitate carrier transport from Si to PEDOT:A film. Based on the aforementioned results, the PEDOT:A film is suitable for constructing Si hybrid devices. Moreover, the devices were fabricated for the first time, the reflectivity of PEDOT:A/Si device was not much different from PEDOT:PSS/Si device in Fig. S4. Achieving an efficiency of 4.62% with a film thickness of 71 nm in Fig. 3c and Fig. S5. The encouraging aspect is that the storage stability of PEDOT:A/Si hybrid solar cells in the air (10%–20% humidity) was superior to that of devices fabricated by PEDOT:PSS, particularly during the initial 50 h in Fig. 3d. Moreover, after storage in the air for 300 h, the PEDOT:A/Si hybrid solar cells retained 90% of their original efficiency, whereas PEDOT:PSS only retained 60% as shown in Table 1 and Table S1. At the same time, the initial performance of PEDOT:PSS device was also shown in Fig. S6. The specific reasons resulting in variations in the stability of different devices were also further discussed in Fig. 4.

To further elaborate on the reasons for the stable performance of PEDOT:A/Si solar cells compared to PEDOT:PSS/Si solar cells, first principles calculations were used to demonstrate the binding

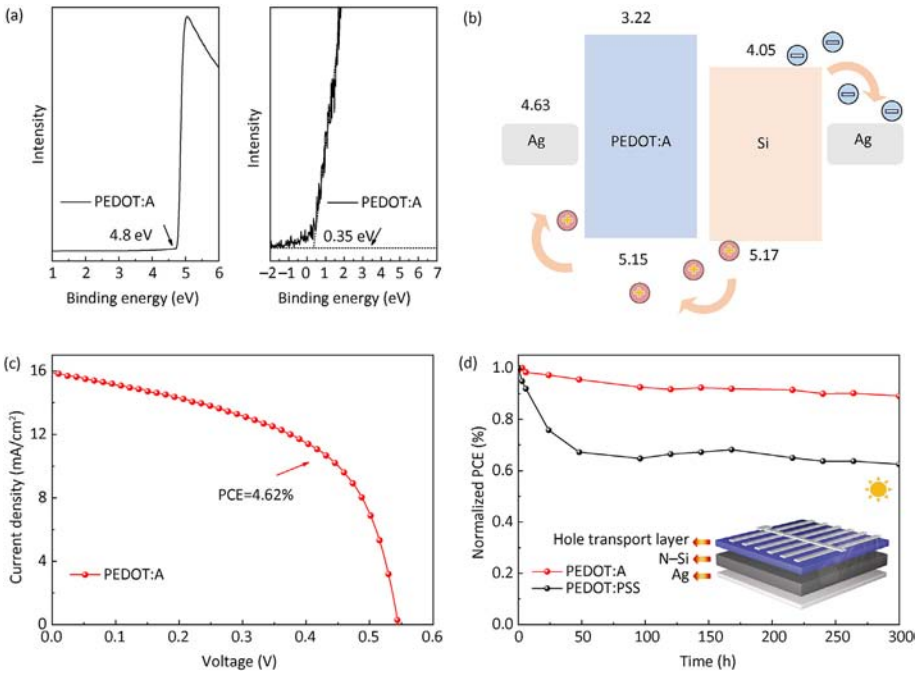

Fig. 3. The photoelectron spectroscopy and schematic diagram of energy level position and performance data of PEDOT:A/Si hybrid solar cells. (a) Ultraviolet photoelectron spectroscopy (UPS) spectra of PEDOT:A film after coordinate change. (b) The schematic diagram for calculating the energy level position of PEDOT:A film according to UPS spectra and absorbance spectrum. (c) Current density–voltage curve of PEDOT:A/Si hybrid solar cells. (d) Normalized PCE varied with time for PEDOT:A/Si hybrid solar cells and PEDOT:PSS/Si hybrid solar cells stored in the air.

Table 1
Electrical output parameters of PEDOT:A/Si solar cells.

	J_{SC} (mA/cm^2)	V_{OC} (V)	FF (%)	PCE (%)
PEDOT:A	15.86 (15.95 ± 0.41)	0.546 (0.55 ± 0.005)	53.35 (53.04 ± 0.87)	4.62 (4.65 ± 0.08)
PEDOT:A-300h	16.57 (16.13 ± 0.89)	0.532 (0.546 ± 0.008)	47.1 (47.7 ± 0.64)	4.15 (4.27 ± 0.13)

*The statistical data are from five sets of solar cell data.

energy between the fluoropolymer-Aquivion, PSS, and water molecule. Because, in the polymerization process of PEDOT derivative, Aquivion or PSS serves as a template that enables the successful dispersion of the resulting polymers. The chemical structures of Aquivion and PSS were shown in Figs. S7a–7b, meanwhile the binding energy between the fluoropolymer-Aquivion, PSS, and water molecule was also shown in Fig. 4b–4c. It was discovered the binding energy between the fluoropolymer-Aquivion, PSS, and water molecule was 3.48 kJ/mol and −5.76 kJ/mol, respectively. Compared to PSS, the interaction between the fluoropolymer-Aquivion and water molecule is weaker, making it difficult for PEDOT:A film to bind with water molecules. Conversely, the strong interaction between PSS and water molecule facilitates the binding of PEDOT:PSS film with water molecules. In addition, the binding energy between fluoropolymer-Nafion, which has the same structure as Aquivion but a different chain length, was also shown in Figs. S7c–d. The binding energy was −4.69 kJ/mol, which also demonstrated that the interaction between the fluoropolymer-Nafion and water molecule was weaker compared to the interaction between PSS and water molecule. Thus, it can be inferred that the CF_2 chains contribute to the low hygroscopicity of the PEDOT:A film. It also can be vividly described in Fig. 4a, when fluoropolymer-Aquivion was introduced to prepare PEDOT:A film, the film seemingly transforms to an umbrella woven by CF_2 chains, effectively shielding the film from the erosion of water molecules. Thus, the degradation of device performance caused by moisture in the air was significantly reduced.

For PEDOT:PSS film, it is easy to combine with water molecules, which results in degradation of device performance. To further verify the hydrophobicity of PEDOT:A film, the contact angle of water on the film was shown in Fig. 4d. The contact angle of water on PEDOT:A film was 100.84°, but the contact angle of water on PEDOT:PSS film was only 38.04° in Fig. 4e. It was suggested that the hydrophobicity of PEDOT:A film was better than PEDOT:PSS film. The contact angle of water on EG-PEDOT:A film was also nearly 100° in Fig. S8, which demonstrates that the hydrophobicity of PEDOT:A film was not influenced after the addition of EG. Surprisingly, when the PEDOT:A film was immersed in water, it remained stable for six days, and even two months, without any decomposition phenomenon in Fig. 4f and Fig. S9. In contrast, when PEDOT:PSS film was immersed in water, it initially disintegrated from the edges and the disintegration proceeded significantly over time. Finally, the film was separated from the substrate surface after 6 min in Fig. 4g. Apart from that, in Figs. S10a–e, the glass and the glass with PEDOT:A film was placed above hot water (67 °C). It was found that, from 0 to 90 s, the blank glass became increasingly blurred due to the continuous coverage of water vapor, whereas the glass coated with PEDOT:A film maintained its clarity throughout. The above results validate the conclusions of the first principles calculations and indicate the excellent hydrophobicity of PEDOT:A film. This is also why the performance of the device can be retained 90% after 300 h in the air.

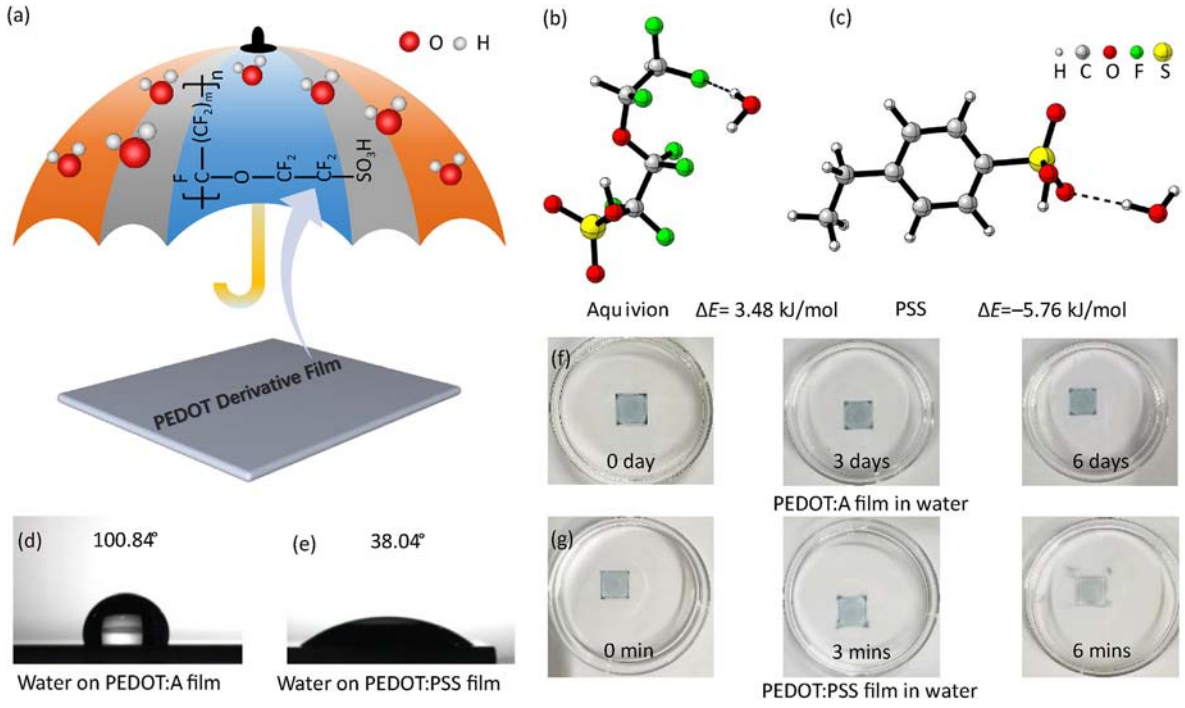

Fig. 4. The diagram of hydrophobic properties of PEDOT derivative film. (a) The hydrophobic characteristic diagram of PEDOT derivative-PEDOT:A film. (b) The binding energy between Aquivion and water molecule. (c) The binding energy between PSS and water molecule. (d) The contact angle of water on PEDOT derivative-PEDOT:A film. (e) The contact angle of water on PEDOT:PSS film. (f) The PEDOT derivative-PEDOT:A film and (g) PEDOT:PSS film immersed in water continuously for different time.

Constructing Si hybrid solar cells with functional materials, without relying on passivation or extra functional layers to assist in improving efficiency, the electric conductivity of film was also a crucial factor. Therefore, a conductive atomic force microscope (AFM) [37] was performed to demonstrate the conductivity of PEDOT:A film. Fig. 5a and c show the conductive AFM current images of PEDOT:A film and PEDOT:PSS film. It can be observed that the image of PEDOT:A is brighter than that of PEDOT:PSS, indicating that the conductivity of PEDOT:A film is slightly better than PEDOT:PSS film. Furthermore, Fig. 5b and d present the current histograms extracted from the conductive AFM current images of PEDOT:A film and PEDOT:PSS film. The mean current for the PEDOT:A film and the PEDOT:PSS film was 34.9 pA and 25.6 pA, respectively.

Meanwhile, the transmission line model method (TLM) was used to measure the electric conductivity (σ) of PEDOT:A and PEDOT:PSS film, as shown in Fig. 6. The schematic diagram of the film resistance test was shown in Fig. S11a. Fig. 6a and b shows the

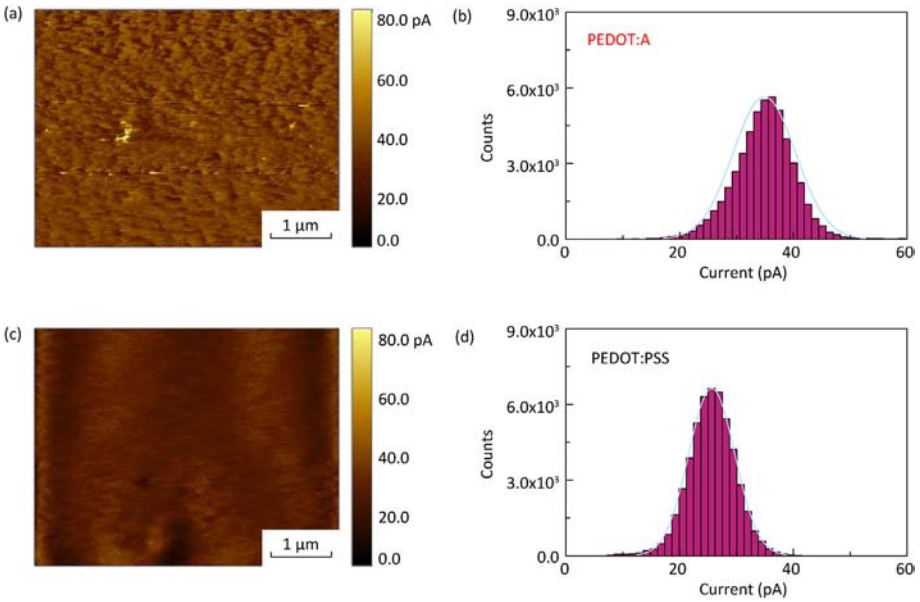

Fig. 5. Conductive AFM current images and current histograms of PEDOT:A and PEDOT:PSS film. (a) Conductive AFM current image of PEDOT:A film surface. (b) Current histogram of PEDOT:A film surface. (c) Conductive AFM current image of PEDOT:PSS film surface. (d) Current histogram of PEDOT:PSS film surface.

dark *I*–*V* characteristic of PEDOT:A and PEDOT:PSS film at silver grid line spacing between 0.2 cm and 0.6 cm. As the spacing between the silver grid lines increases, the resistance of the film between the silver grid lines increases, and the current decreases. Thus, the resistance of the PEDOT:A film and PEDOT:PSS film for different widths can be calculated from Fig. 6a–6b. The resistance of the PEDOT:A and PEDOT:PSS film at different spacings were also shown in Fig. 6c–6d, respectively. It can be seen that the resistance of PEDOT:A film was all below 2.66×10^7 Ω and the resistance of PEDOT:PSS film was all above 3.2×10^7 Ω, which suggests that the resistance of PEDOT:A film is smaller than PEDOT:PSS film. By linearly fitting the resistance obtained from different distances, the slope is the resistance per unit width of film. Therefore, the electric conductivity of the film can be obtained through formula (2), and the specific formula is as follows:

$$\sigma = \frac{1}{\rho \times A \times h} \tag{2}$$

where σ is the electric conductivity of the film, ρ is the resistance per unit width of the film, A is the length of the silver grid line, which was 1.7 cm, and h is the thickness of the PEDOT:A film and PEDOT:PSS film, as shown in Figs. S11b–11c. The results of ρ and electric conductivity of PEDOT:A and PEDOT:PSS film are calculated in Fig. 6e and f, where PEDOT:A has an electric conductivity of 1.59×10^{-3} S/cm, and PEDOT:PSS has an electric conductivity of 2.71×10^{-4} S/cm. This shows that the electric conductivity of the PEDOT:A film is comparable to or even slightly higher than PEDOT:PSS film. It also indicates from the perspective of electrical properties that the PEDOT:A film was suitable for constructing devices.

3.4. Performance improved of PEDOT:A/Si hybrid solar cells

In order to further improve the efficiency of PEDOT:A/Si hybrid solar cells, ITO layer was deposited on PEDOT:A film to enhance the lateral carrier collection ability. Notably, after the deposition of the ITO layer on PEDOT:A film, the short-circuit current density (J_{SC}) of the device was increased from 15.86 mA/cm^2 to 19 mA/cm^2, and the fill factor (FF) was also improved, as shown in Fig. 7a. At the same

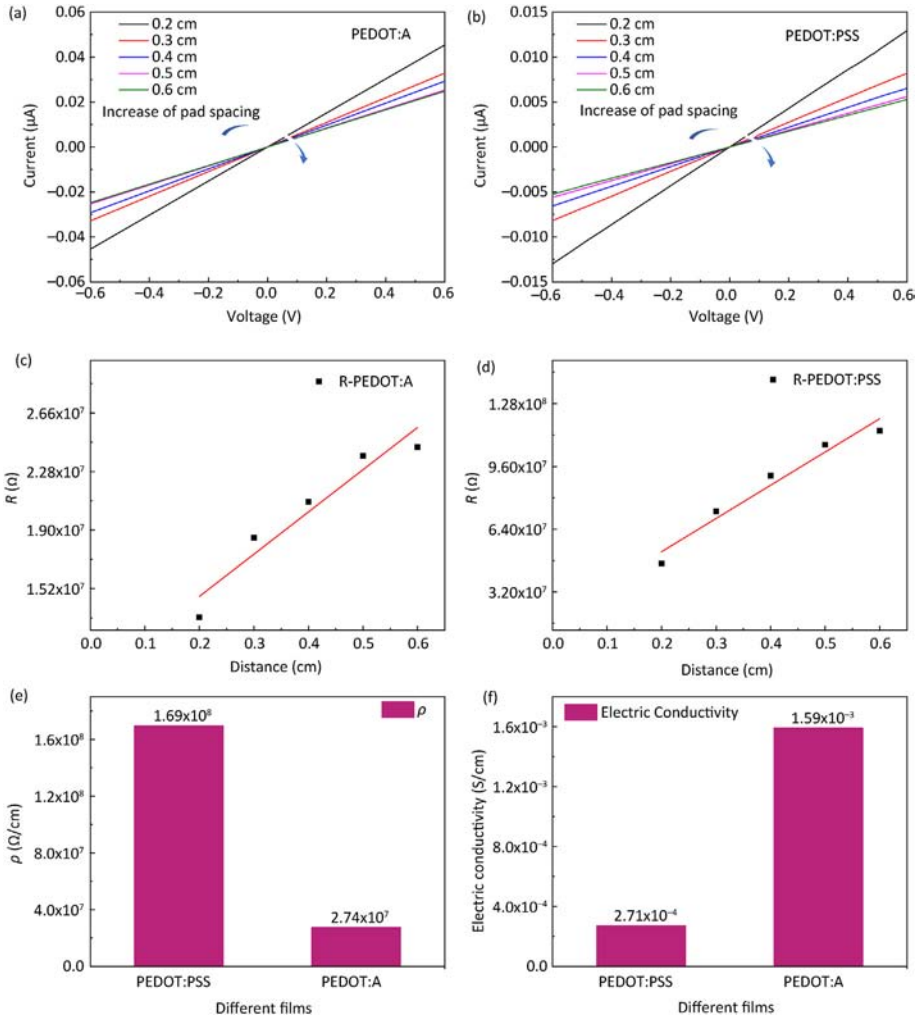

Fig. 6. Electric conductivity of PEDOT:A and PEDOT:PSS film. (a) Dark *I-V* characteristics of PEDOT:A film and (b) PEDOT:PSS film on glass. (c) Measured resistance of PEDOT:A film and (d) PEDOT:PSS film as a function of channel length. (e)The value of ρ of different films by fit slope. (f) The value of electric conductivity of different films.

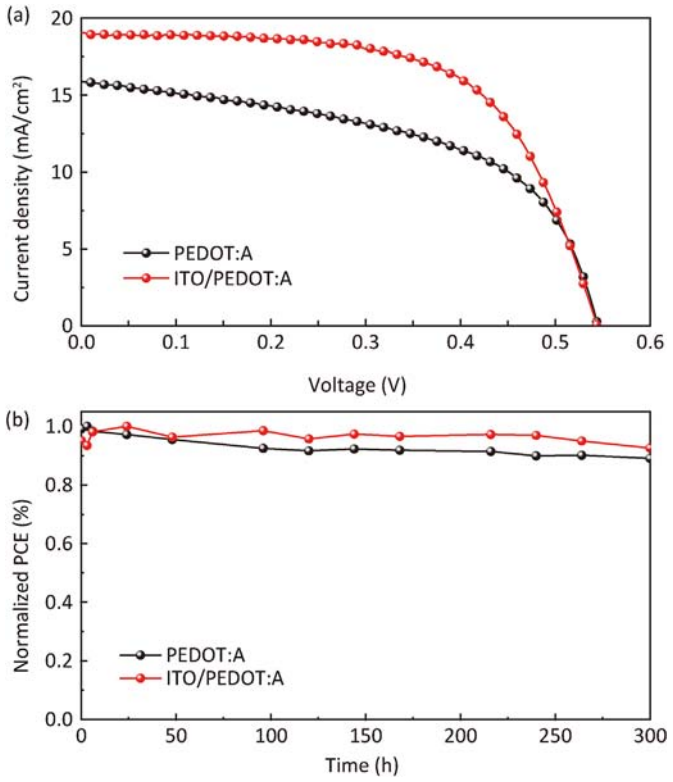

Fig. 7. Performance of ITO/PEDOT:A/Si hybrid solar cells. (a) Current density-voltage curve of ITO/PEDOT:A/Si hybrid solar cells. (b) Normalized PCE varied with time for ITO/PEDOT:A/Si hybrid solar cells and PEDOT:A/Si hybrid solar cells stored in the air.

Table 2
Electrical output parameters of ITO/PEDOT:A/Si solar cells.

	J_{SC} (mA/cm^2)	V_{OC} (V)	FF (%)	PCE (%)
ITO/PEDOT:A	19 (18.71 ± 0.22)	0.543 (0.54 ± 0.003)	62.25 (62.74 ± 1.07)	6.43 (6.35 ± 0.08)
ITO/PEDOT:A-300h	18.92 (18.75 ± 0.20)	0.536 (0.543 ± 0.005)	61.64 (61.67 ± 1.76)	6.26 (6.25 ± 0.22)

*The statistical data are from five sets of solar cell data.

time, we also monitored the stability of the device with ITO, and detected that its stability performance remains satisfactory. As shown in Fig. 7b, after storage in the air for 300 h, the PEDOT:A/Si hybrid solar cells retained 97% of its initial efficiency, decreasing only from 6.43% to 6.26%, as indicated in Table 2.

4. Conclusions

With the introduction of fluoropolymer, the PEDOT derivative, PEDOT:A, was prepared, and the PEDOT:A/Si solar cells were constructed using a hydrophobic PEDOT:A film. Research has found that the contact angle of PEDOT:A solution on the Si surface was only 16.47°, achieving easy film-forming and high film quality. Meanwhile, the positions of the conduction and valence band energy level of the PEDOT:A film are 3.22 eV and 5.15 eV, which can achieve a good match with that of Si. The PEDOT:A/Si solar cells retained 90% of its initial performance after a 300 h device storage stability test compared to 60% of PEDOT:PSS. Meanwhile, first principles calculations revealed that the binding energies between fluoropolymer-Aquivion, PSS, and water molecule were 3.48 kJ/mol and −5.76 kJ/mol, respectively. Profiting from the weak interaction between fluoropolymer and water molecule, the contact angle of water on the PEDOT:A film exceeds 100°, thus the film can remain stable in water for a long period without dissolution. Through the use of ITO, the PCE of PEDOT:A/Si hybrid solar cells was 6.43%, decay 3% of its initial efficiency after monitoring under identical conditions. This also facilitates the practical applications of low-cost Si based solar cells due to the technology development of air-stable Si hybrid solar cells.

Data availability

Data will be made available on request.

CRediT authorship contribution statement

Qi Geng: Writing – original draft. **Zhen Liu:** Investigation. **Yuzhou Liu:** Methodology. **Zhe Wang:** Methodology. **Zhongliang Gao:** Formal analysis. **Xin Sun:** Formal analysis. **Yingfeng Li:** Formal analysis. **Lei Chen:** Formal analysis. **Xiaojun Lv:** Conceptualization. **Meicheng Li:** Supervision.

Declaration of competing interest

The authors declare that they have no known competing financial interests or personal relationships that could have appeared to influence the work reported in this paper.

Acknowledgments

This work is supported partially by National Natural Science Foundation of China (Grant nos. 52232008, 51972110, 52102245, 62304125, and 52072121), Beijing Natural Science Foundation (2222076, 2222077), Beijing Science and Technology Project (Z211100004621010), project of State Key Laboratory of Alternate Electrical Power System with Renewable Energy Sources(LAPS2024-05), 2022 Strategic Research Key Project of Science and Technology Commission of the Ministry of Education, Huaneng Group Headquarters Science and Technology Project (HNKJ20-H88), the Fundamental Research Funds for the Central Universities (2022MS029, 2022MS02, 2022MS031) and the NCEPU "Double First-Class" Program.

Appendix A. Supplementary data

Supplementary data to this article can be found online at https://doi.org/10.1016/j.jmat.2024.100935.

References

[1] Wang J, Zhou W, Wei Q, Liu G, Yuan X, Pen H, et al. Effect of Au@MoS_2 contacted PEDOT:PSS on work function of planar silicon hybrid solar cells. Adv Mater Interfac 2023;10:2300187.
[2] Ni Z, Ding S, Zhang H, Dai R, Chen A, Wang R, et al. Phosphorus and selenium co-doped WO_3 nanoparticles for interface modification and photovoltaic properties enhancement of monolayer planar silicon/PEDOT:PSS hybrid solar cells. Adv Mater Interfac 2022;9:2200812.
[3] Xu Q, Song T, Cui W, Liu Y, Xu W, Lee ST, et al. Solution-processed highly conductive PEDOT:PSS/AgNW/GO transparent film for efficient organic-si hybrid solar cells. ACS Appl Mater Interfaces 2015;7:3272–9.
[4] Liu J, Ji Y, Liu Y, Xia Z, Han Y, Li Y, et al. Doping-free asymmetrical silicon heterocontact achieved by integrating conjugated molecules for high efficient solar cell. Adv Energy Mater 2017;7:1700311.
[5] Liu H, Jiang W, Fan Z, An Y, Wei G, Li Y, et al. Interfacial band engineering of highly efficient PEDOT:PSS/p-Si/ZnO heterojunction solar cells. Sol RRL 2024;8:2400119.
[6] Zhu J, Yang X, Sheng J, Gao P, Ye J. Double-layered PEDOT:PSS films inducing strong inversion layers in organic/silicon hybrid heterojunction solar cells. ACS Appl Energy Mater 2018;1:2874–81.
[7] Yu L, Chen T, Feng N, Wang R, Sun T, Zhou Y, et al. Highly conductive and wettable PEDOT:PSS for simple and efficient organic/c-Si planar heterojunction solar cells. Sol RRL 2020;4:1900513.

[8] Yang C, Luo Z, Ma W, Li S, Lv G, Fu K, et al. Study on the fabrication of PEDOT:PSS/Si hybrid solar cells incorporated with F4TCNQ and VTMO. J Phys Chem C 2023;127:7974–86.
[9] He J, Gao P, Yang Z, Yu J, Yu W, Ye J, et al. Silicon/organic hybrid solar cells with 16.2% efficiency and improved stability by formation of conformal heterojunction coating and moisture-resistant capping layer. Adv Mater 2017;29:1606321.
[10] Yoon S-S, Kang D-Y. High efficiency (>17%) Si-organic hybrid solar cells by simultaneous structural, electrical, and interfacial engineering *via* low-temperature processes. Adv Energy Mater 2017;8:1702655.
[11] Lu Z, Zhu Y, Chen J, Hou G, Song H, Xu J, et al. Over 16% efficiency organic/nanostructured Si heterojunction solar cells with a p-doped organic small molecule layer. Org Electron 2022;108:106576.
[12] Zielkea D, Niehaves C, Lövenichb W, Elschnerb A, Hörteisb M, Schmidt J. Organic-silicon solar cells exceeding 20% efficiency. Energy Proc 2015;77:331–9.
[13] Luo Z, Yang C, Chen X, Ma W, Li S, Fu K. Improving open-circuit voltage and short-circuit current of high efficiency silicon-based planar heterojunction solar cells by combining V_2O_5 with PEDOT:PSS. Journal of Materiomics 2022;9:438–46.
[14] Shen R, Sun Z, Zhou Y, Shi Y, Shang J, Chen H, et al. Organic/silicon nanowires hybrid solar cells using isobutyltriethoxysilane incorporated poly(3,4-ethylenedioxythiophene):poly (styrenesulfonate) as hole transport layer. Prog Photovoltaics 2022;30:661–9.
[15] Thomas JP, Rahman MA, Srivastava S, Kang JS, Mcgillivray D, Abd-Ellah M, et al. Highly conducting hybrid silver-nanowire-embedded Poly(3,4-ethylenedioxythiophene):Poly(styrenesulfo nate) for high-efficiency planar silicon/organic heterojunction solar cells. ACS Nano 2018;12:8833–9634.
[16] Sharma D, Srivastava A, Tawale JS, Prathap P, Srivastava SK. High efficiency flexible PEDOT:PSS/silicon hybrid heterojunction solar cells by employing simple chemical approaches. J Mater Chem C 2023;11:13488–502.
[17] Gao Z, Gao T, Geng Q, Lin G, Li Y, Chen L, et al. Improving light absorption of active layer by adjusting PEDOT:PSS film for high efficiency Si-based hybrid solar cells. Sol Energy 2021;228:299–307.
[18] Yu L, Man J, Chen T, Luo D, Wang J, Yang H, et al. Colorful conducting polymers for vivid solar panels. Nano Energy 2021;85:105937.
[19] Zhu J, Xu Y, Luo Y, Luo J, He R, Wang C, et al. Custom-tailored hole transport layer using oxalic acid for high-quality tin-lead perovskites and efficient all-perovskite tandems. Sci Adv 2024;10:eadl2063.
[20] Cao F, Wu Q, Yang X. Yang Efficient and stable inverted quantum dot light-emitting diodes enabled by an inorganic copper-doped tungsten phosphate hole-injection layer. ACS Appl Mater Interfaces 2019;11:40267–73.
[21] Cao F, Wu Q, Sui Y, Wang S, Dou YJ, Hua W, et al. All-inorganic quantum dot light-emitting diodes with suppressed luminance quenching enabled by chloride passivated tungsten phosphate hole transport layers. Small 2021;17:2100030.
[22] Chen H, Li C. PEDOT: fundamentals and its nanocomposites for energy storage. Chin J Polym Sci 2020;38:435–48.
[23] Liu R, Wang J, Sun T, Wang M, Wu C, Zou H, et al. Silicon nanowire/polymer hybrid solar cell-supercapacitor: a self charging power unit with a total efficiency of 10.5. Nano Lett 2017;17:4240–7.
[24] Zhuang B, Wang X, Zhang Q, Liu J, Jin Y, Wang H. Nanoengineering of poly(3,4-ethylenedioxythiophene) for boosting electrochemical applications. Sol Energy Mater Sol Cells 2021;232:111357.
[25] Petsagkourakis I, Kim N, Tybrandt K, Zozoulenko I, Crispin X. Poly(3,4-ethylenedioxythiophene): chemical synthesis, transport properties, and thermoelectric devices. Adv Electron Mater 2019;5:1800918.
[26] Kurushima Y, Katsuyama N, Okuzaki H. Effect of PEDOT:PSS composition on photovoltaic performance of PEDOT:PSS/n-Si hybrid solar cells. Jpn J Appl Phys 2021;60:091001.
[27] Liu H, Liu Q, Liu J, Zhao Y, Yu Y, An Y, et al. Effects of different interface on the stability of hybrid heterojunction solar cells. Sol Energy Mater Sol Cells 2024;264:112624.
[28] He L, Jiang C, Lai D, Wang H. Rusli. Enhanced conversion efficiency for Si nanowire-organic hybrid solar cells through the incorporation of organic small molecule, Jpn. J Appl Phys 2012;51:10NE36.
[29] He J, Gao P, Ling Z, Ding L, Yang Z, Ye J, et al. High-efficiency silicon/organic heterojunction solar cells with improved junction quality and interface passivation. ACS Nano 2016;10:11525–31.
[30] Jiang L, Zhou Z, Zhang G, Li C, Feng Q, Wei Q, et al. Waterborne acrylic resin-modified PEDOT:PSS as a hole transporting layer for silicon/organic solar cells with improved efficiency and stability. ACS Appl Energy Mater 2024;7:3927–36.
[31] Subramani T, Chen J, Kobayashi Y, Jevasuwan W, Fukata N. Highly air-stable solution-processed and low-temperature organic/inorganic nanostructure hybrid solar cells. ACS Appl Energy Mater 2019;2:2637–44.
[32] Shi W, Yao Q, Qu S, Chen H, Zhang T, Chen L. Micron-thick highly conductive PEDOT films synthesized *via* self-inhibited polymerization: roles of anions. NPG Asia Mater 2017;9:e405.
[33] Chen R, Sun k, Zhang Q, Zhou Y, Li M, Sun Y, et al. Sequential solution polymerization of Poly(3,4ethylenedioxythiophene) using V_2O_5 as oxidant for flexible touch sensors. iScience 2019;12:66–75.
[34] Hofmann AI, Katsigiannopoulos D, Mumtaz M, Petsagkourakis I, Pecastaings G, Fleury G, et al. How to choose polyelectrolytes for aqueous dispersions of conducting PEDOT complexes. Macromolecules 2017;50:1959–69.
[35] Jiang Y, Dong X, Sun L, Liu T, Qin F, Xie C, et al. An alcohol-dispersed conducting polymer complex for fully printable organic solar cells with improved stability. Nat Energy 2022;7:352–9.
[36] Carli S, Di Lauro M, Bianchi M, Murgia M, De Salvo A, Prato M, et al. Water-based PEDOT:Nafion dispersion for organic bioelectronics. ACS Appl Mater Interfaces 2020;12:29807–17.
[37] Li W, Zhang X, Zhang X, Yao J, Zhan C. High-performance solution-processed single-junction polymer solar cell achievable by post-treatment of PEDOT:PSS layer with water containing methanol. ACS Appl Mater Interfaces 2017;9:1446–52.

Qi Geng is currently a Ph.D. Candidate majored in Renewable and Clean Energy at School of New Energy, North China Electric Power University. His research focuses on Si-based solar cells.

Prof. Meicheng Li is the Dean of School of New Energy in North China Electric Power University. His current research topic is the New Energy Materials and Devices, focusing on the nanostructures of silicon, perovskite, carbon and oxide *etc*, and the relative novel device applications in energy harvesting, conversion, and storage, such as solar cells, lithium/sodium ion battery, and other solar devices, sensors, *etc*.